

Effects of excitons on solar cells

Yong Zhang,^{a)} Angelo Mascarenhas, and Satyen Deb

National Renewable Energy Laboratory, Golden, Colorado 80401

(Received 1 May 1998; accepted for publication 6 July 1998)

We have studied the effects of excitons on the two key parameters of a Si solar cell: the dark-saturation current and short-circuit current. We have found that the effect of excitons on the dark-saturation current is very sensitive to the boundary condition for excess excitons at the edge of the depletion region. With the assumption of near equilibrium between the electrons and excitons, we find that the exciton effect is rather small, which is contrary to the conclusion of significant reduction in the dark-saturation current made in previous work with the assumption of no excess excitons at the edge [J. Appl. Phys. **79**, 195 (1996)]. The results for the short-circuit current are very similar to the previous work. However, the analytical results for the carrier concentrations and the corresponding currents are now presented in a simple way in which the physical meaning of each individual term is elucidated or revealed. Furthermore, we have found, for practical purposes, very accurate approximate solutions for the carrier concentrations and corresponding currents. Our conclusion is that the major effect of excitons on the Si solar cell performance relies on whether the effective diffusion length (L_1) of the coupled electron–exciton system is significantly greater than that of the electron itself (L_e). © 1998 American Institute of Physics. [S0021-8979(98)05519-4]

I. INTRODUCTION

In a conventional theory for the operation of a semiconductor photovoltaics device at room temperature or above, only the generation, recombination, and transport of free carriers, electrons and holes, are taken into account. However, it has been pointed out that the free exciton density in silicon at room temperature can approach the density of minority carriers.^{1,2} Thus, the role of free excitons in the device operation may be significant, which has been demonstrated theoretically by Kane and Swanson² and Corkish, Chan, and Green³ for silicon devices. The effects of excitons can be summarized as having two benefits for a silicon solar cell:³ a significant decrease in dark-saturation current, and a simultaneous increase in short-circuit current, if the exciton diffusion length exceeds that for minority carriers.

In this work, we re-examine the effects of excitons in a silicon solar cell. As in Ref. 3, we consider a simplified solar cell model, that is, an n^+p “one-sided” junction model (the thin emitter layer is ignored and only the base region is considered). Also, we adopted the following approximations made in Ref. 3: (1) the depletion approximation; (2) within the depletion region, the drift and diffusion currents are opposing and approximately equal in magnitude; (3) low-level injection is assumed; (4) minority carriers in the bulk regions are assumed to flow predominantly by diffusion; (5) recombination in the depletion region is neglected. An extra assumption was made in Ref. 3: the number of the minority carriers at the edge of the depletion region on the base side equals that of the injected carriers (i.e., no excitons are formed at the edge). This assumption causes an abrupt change (increase) in the exciton distribution as soon as one moves away from the edge, which, in turn, gives a large

opposite diffusion current to that given by the normal minority carrier diffusion, thus resulting in a significant reduction of the dark-saturation current. Because there is no obvious reason to forbid the formation of the exciton at the edge, in this work we assume that the carriers and excitons are in quasi-equilibrium. With our assumption, the effect of excitons on the dark-saturation current is much smaller than expected in the previous model. Analytical solutions for the electron and exciton concentrations, as well as the formulae for the relevant currents, are presented in greatly simplified but physically more revealing ways, which leads to very accurate approximate solutions or formulae for the case of a relatively large exciton binding coefficient.

II. MODEL

For the simplified solar cell model, distributions of the excess minority carriers (Δn_e) and excess excitons (Δn_x) in the p -type layer can be described by the following coupled differential equations:³

$$D_e \frac{d^2 \Delta n_e}{dz^2} = \frac{\Delta n_e}{\tau_e} + b(\Delta n_e N_A - \Delta n_x n^*) - G_e \exp(-\alpha z), \quad (1)$$

$$D_x \frac{d^2 \Delta n_x}{dz^2} = \frac{\Delta n_x}{\tau_x} - b(\Delta n_e N_A - \Delta n_x n^*) - G_x \exp(-\alpha z), \quad (2)$$

where D is the diffusion coefficient, τ is the lifetime, G is the generation rate, and α is the absorption coefficient. Subscripts e and x stand for electron and exciton, respectively. N_A is the concentration of the p -type doping, n^* is an equilibrium constant (in equilibrium, $n_e n_h = n_x n^*$), and b is a

^{a)}Electronic mail: yzhang@nrel.gov

coefficient for binding of carriers into excitons. The $z=0$ plane is defined at the p -type edge of the depletion region.

If the electron–exciton exchange is ignored, the excess electron distribution is given as

$$\Delta n_e(z) = \Delta n_e(0) \exp(-z/L_e) + \frac{G_e}{(L_e^{-2} - \alpha^2)D_e} \times [\exp(-\alpha z) - \exp(-z/L_e)], \quad (3)$$

where $L_e = \sqrt{D_e \tau_e}$ is the electron diffusion length. The first and second terms on the right describe the diffusion of injected and photogenerated carriers, respectively. The solution for excitons is the same as Eq. (3) except for changing the subscript e to x , and the exciton diffusion length is defined as $L_x = \sqrt{D_x \tau_x}$. Equation (3) would be the carrier distribution used in the conventional device theory without considering excitons.

Following Ref. 3, we write Eqs. (1) and (2) in matrix form,

$$\frac{d^2}{dz^2} \begin{pmatrix} \Delta n_e \\ \Delta n_x \end{pmatrix} = \begin{pmatrix} M_{11} & M_{12} \\ M_{21} & M_{22} \end{pmatrix} \begin{pmatrix} \Delta n_e \\ \Delta n_x \end{pmatrix} + \begin{pmatrix} \Gamma_e(z) \\ \Gamma_x(z) \end{pmatrix}, \quad (4)$$

where

$$\begin{aligned} M_{11} &= (1/\tau_e + bN_A)/D_e, \\ M_{22} &= (1/\tau_x + bn^*)/D_x, \\ M_{12} &= -bn^*/D_e, \\ M_{21} &= -bN_A/D_x, \\ \Gamma_e(z) &= -G_e \exp(-\alpha z)/D_e, \end{aligned}$$

and

$$\Gamma_x(z) = -G_x \exp(-\alpha z)/D_x.$$

Matrix $M = \{M_{ij}\}$ has two eigenvalues:

$$\begin{aligned} \epsilon_1 &= \frac{M_{11} + M_{22} - \sqrt{\delta}}{2}, \\ \epsilon_2 &= \frac{M_{11} + M_{22} + \sqrt{\delta}}{2}, \end{aligned}$$

where $\delta = M_{\Delta}^2 + 4M_{12}M_{21}$, and $M_{\Delta} = M_{11} - M_{22}$. There are two characteristic “diffusion” lengths associated with Eq. (4) for the coupled electron–exciton system. They are $L_1^{-1} = \sqrt{\epsilon_1}$ and $L_2^{-1} = \sqrt{\epsilon_2}$. Introducing a transform P ,³ such that

$$P^{-1}MP = \begin{pmatrix} \epsilon_1 & 0 \\ 0 & \epsilon_2 \end{pmatrix},$$

and

$$\begin{pmatrix} \Delta n_e \\ \Delta n_x \end{pmatrix} = P \begin{pmatrix} \Delta n_1 \\ \Delta n_2 \end{pmatrix}.$$

P can be chosen to be (with this choice of P , $\Delta n_1 > 0$, and $\Delta n_2 > 0$)

$$P = - \begin{pmatrix} M_{12} & M_{12} \\ \epsilon_1 - M_{11} & \epsilon_2 - M_{11} \end{pmatrix}.$$

We first define a function

$$F(L, D, G) = \frac{G}{(L^{-2} - \alpha^2)D} [\exp(-\alpha z) - \exp(-z/L)],$$

which describes the diffusion-induced distribution of photo-generated carriers with a diffusion length L and a diffusion coefficient D under a generation rate G . The general solutions can be presented as follows:

$$\begin{aligned} \Delta n_1 &= c_{11} [n_{e0} \exp(-z/L_1) + F(L_1, D_e, G_e)] \\ &\quad + c_{12} [n_{x0} \exp(-z/L_1) + F(L_1, D_x, G_x)], \end{aligned} \quad (5)$$

$$\begin{aligned} \Delta n_2 &= c_{21} [n_{e0} \exp(-z/L_2) + F(L_2, D_e, G_e)] \\ &\quad + c_{22} [n_{x0} \exp(-z/L_2) + F(L_2, D_x, G_x)], \end{aligned} \quad (6)$$

where $\Delta n_{e0} = \Delta n_e(z=0)$ and $\Delta n_{x0} = \Delta n_x(z=0)$, and

$$c_{11} = - \frac{\sqrt{\delta} - M_{\Delta}}{2M_{12}\sqrt{\delta}},$$

$$c_{12} = \frac{1}{\sqrt{\delta}},$$

$$c_{21} = - \frac{\sqrt{\delta} + M_{\Delta}}{2M_{12}\sqrt{\delta}},$$

and

$$c_{22} = - \frac{1}{\sqrt{\delta}}.$$

Compared to Eq. (3), the physical interpretation for each individual term in Eqs. (5) and (6) is straightforward. For instance, $F(L_1, D_e, G_e)$ describes how the photogenerated electrons diffuse with a diffusion coefficient D_e but with a diffusion length L_1 . Coefficients c_{ij} describe the coupling between the electron and exciton systems. The solutions for the electrons and excitons are then given by

$$\Delta n_e = -M_{12}(\Delta n_1 + \Delta n_2), \quad (7)$$

and

$$\Delta n_x = (M_{11} - \epsilon_1)\Delta n_1 + (M_{11} - \epsilon_2)\Delta n_2. \quad (8)$$

We now consider the relative scale of two characteristic lengths L_1 and L_2 . Figure 1 shows L_1 and L_2 as a function of the exciton binding coefficient b , compared to the electron and exciton diffusion lengths L_e and L_x . As expected, when b is very small, electrons and excitons diffuse independently, with $L_1 \approx L_x$ and $L_2 \approx L_e$. When b is large enough, $L_x > L_1 > L_e$ and $L_2 \rightarrow 0$. Material parameters used for calculating L and other properties later in this article are listed in Table I. These parameters are essentially the same as those used in Ref. 3.

III. RESULTS AND DISCUSSIONS

A. Dark-saturation current

The dark-saturation current is the cell current under a forward bias V and without illumination. The number of the injected excess electrons is assumed to be $\Delta n_0 = n_{p0}[\exp(qV/kT) - 1]$, where $n_{p0} \approx n_i^2/N_A$ (the equilibrium

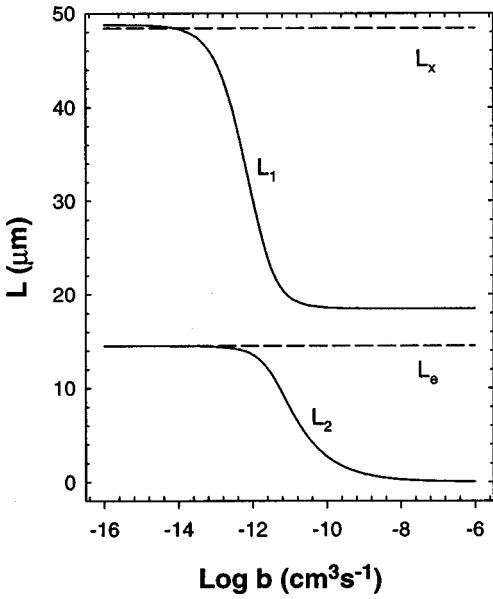


FIG. 1. Two characteristic diffusion lengths L_1 and L_2 for the coupled electrons–excitons system as a function of the exciton binding coefficient b at doping level $N_A = 5 \times 10^{15} \text{ cm}^{-3}$, compared to the electron and exciton diffusion lengths L_e and L_x .

minority carrier concentration in the p -type region) and n_i is the intrinsic carrier concentration. We have assumed the total number of the injected electrons is the same Δn_0 even with the existence of excitons. However, we allow these injected electrons either to form excitons or remain in the conduction band anywhere outside of the depletion region, including at $z=0$ (while in Ref. 3, it was implicitly assumed that all the electrons at $z=0$ remained in the conduction band). The solutions of Eq. (4) in the dark condition is given explicitly as follows:

$$\Delta n_e(z) = \frac{1}{2\sqrt{\delta}} \{ [(\sqrt{\delta} - M_\Delta)\Delta n_{e0} - 2M_{12}\Delta n_{x0}] \times \exp(-z/L_1) + [(\sqrt{\delta} + M_\Delta)\Delta n_{e0} + 2M_{12}\Delta n_{x0}] \exp(-z/L_2) \}, \quad (9)$$

TABLE I. Parameters and formulae used in this article.^a

Parameters	Values or formulae
Electron lifetime $\tau_e(0)$	$1.70 \times 10^{-5} \text{ s}$
$\tau_e(N_A)$	$\tau_e(0)/(1 + N_A/7.10 \times 10^{15}) \text{ s}$
Exciton lifetime $\tau_x(0)$	10^{-4} s
$\tau_x(N_A)$	$\tau_x(0)/(1 + N_A/7.10 \times 10^{15}) \text{ s}$
Exciton binding energy $E_{x\infty}$	20.6 meV
Mott density n_{Mott}	$1.03 \times 10^{18} \text{ cm}^{-3}$
$E_x(N_A)$	$E_{x\infty}[1 - (N_A/n_{\text{Mott}})^{1/2}]^2 \text{ meV}$
Equilibrium constant n^*	$\exp[-E_x(N_A)/kT] 1.43 \times 10^{18} \text{ cm}^{-3}$
Electron diffusion coefficient $D_e(N_A)$	$0.02586\{65 + 1265/[1 + (N_A \times 10^{-16}/8.5)^{0.72}]\} \text{ cm}^2 \text{ s}^{-1}$
Exciton diffusion coefficient D_x	$17 \text{ cm}^2 \text{ s}^{-1}$
Absorption coefficient α	0 cm^{-1}

^aReference 3.

$$\Delta n_x(z) = \frac{1}{2\sqrt{\delta}} \{ [(\sqrt{\delta} + M_\Delta)\Delta n_{x0} - 2M_{21}\Delta n_{e0}] \times \exp(-z/L_1) + [(\sqrt{\delta} - M_\Delta)\Delta n_{x0} + 2M_{21}\Delta n_{e0}] \exp(-z/L_2) \}. \quad (10)$$

If one assumes $\Delta n_{x0} = 0$, Eqs. (9) and (10) will be simplified to Eqs. (12) and (13) in Ref. 3.

The dark-saturation current can be calculated as³

$$j_{\text{dsc}} = qD_e \left. \frac{d\Delta n_e}{dz} \right|_{z=0} + qD_x \left. \frac{d\Delta n_x}{dz} \right|_{z=0} = -qD_e \Delta n_{e0} \left(\frac{\eta}{L_1} + \frac{1-\eta}{L_2} \right) - qD_x \Delta n_{x0} \left(\frac{\zeta}{L_1} + \frac{1-\zeta}{L_2} \right), \quad (11)$$

where

$$\eta = \frac{1}{2} - \frac{M_\Delta + 2M_{21}D_x/D_e}{2\sqrt{\delta}},$$

$$\zeta = \frac{1}{2} + \frac{M_\Delta - 2M_{12}D_e/D_x}{2\sqrt{\delta}}.$$

The dark-saturation current without considering excitons is

$$j_{\text{dsc}0} = qD_e \left. \frac{d\Delta n_e}{dz} \right|_{z=0} = -\frac{qD_e \Delta n_0}{L_e}. \quad (12)$$

Equation (11) can be understood as that the dark-saturation current has contributions from both electrons and excitons; and for either electrons or excitons, some of them diffuse with a diffusion length L_1 and the rest of them diffuse with a diffusion length L_2 . When b is small, $\eta \rightarrow 0$ and $\zeta \rightarrow 1$, $L_1 \rightarrow L_e$ and $L_2 \rightarrow L_x$, so $j_{\text{dsc}} \approx -q(D_e \Delta n_{e0}/L_e + D_x \Delta n_{x0}/L_x)$, implying that electrons and excitons diffuse independently with their own characteristics. Whether or not consideration of the exciton contribution leads to a reduction of the dark-saturation current depends on whether or not the condition $D_e \Delta n_0/L_e > D_e \Delta n_{e0}/L_e + D_x \Delta n_{x0}/L_x$ is satisfied. When b is large, $\eta \rightarrow 1$, $\zeta \rightarrow 1$, so $j_{\text{dsc}} \approx -q(D_e \Delta n_{e0} + D_x \Delta n_{x0})/L_1$. The contribution of the L_2 -related terms is negligible, which is physically reasonable because of the small diffusion length for the L_2 component for large b . The condition for the reduction of the dark-saturation current is then $(D_e \Delta n_{e0} + D_x \Delta n_{x0})/L_1 < D_e \Delta n_0/L_e$. Although $L_1 > L_e$ is favorable, $D_x > D_e$ is unfavorable for reducing the dark-saturation current. If the boundary condition $\Delta n_{x0} = 0$ is assumed, it follows trivially that for large b , the exciton effect will reduce the dark-saturation current simply because of $L_1 > L_e$, as shown numerically in Ref. 3. However, $\Delta n_{x0} = 0$ is not a well-justified assumption. Because the electric field is zero at the edge of the depletion region, the excitons should be allowed to co-exist with the electrons and holes. Although it is not trivial to determine this boundary condition, here we consider another extreme situation, which is that at the edge of the depletion region, the condition

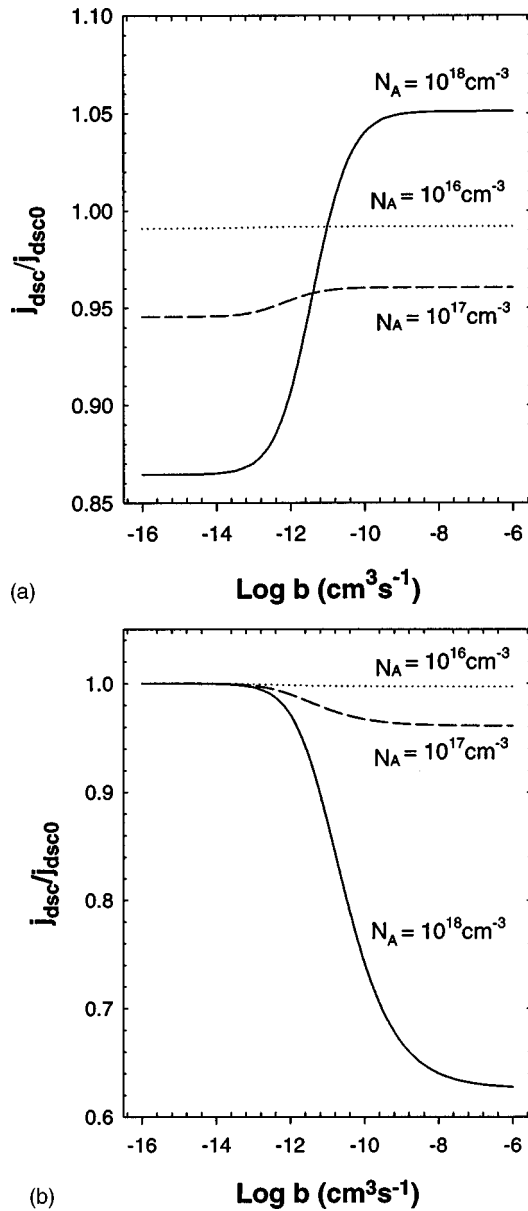


FIG. 2. Ratio of dark-saturation current density with excitons considered to that with excitons neglected as a function of the exciton binding coefficient at three doping levels: $N_A = 10^{16}$, 10^{17} , and 10^{18} cm^{-3} , assuming (a) $N_A \Delta n_e(0) = n^* \Delta n_x(0)$, and (b) $\Delta n_x(0) = 0$.

$n^* \Delta n_{x0} = N_A \Delta n_{e0}$ is satisfied. Figure 2(a) shows the ratio of the dark-saturation currents with and without consideration of excitons at a few different doping levels. The results using the new assumption for Δn_{x0} show very little effect of excitons for large b , and a weak reduction in the dark-saturation current for small b . For comparison, Fig. 2(b) shows the results using Ref. 3's assumption, where the exciton effect significantly reduces the dark-saturation current at high doping levels for large b .

The validity of the new boundary condition lies in the fact that the exciton formation time $(bN_A)^{-1}$ and the exciton thermal disassociation time $(bn^*)^{-1}$ are much shorter than the electron lifetime τ_e and the exciton lifetime τ_x , respectively. For a reasonably large value of b ($b > 10^{-10} \text{ cm}^3 \text{ s}^{-1}$), we find that the relation $|N_A \Delta n_e$

$-n^* \Delta n_x|/(N_A \Delta n_e) \ll 1$ remains true for $z > 0$, independent of which boundary condition is used. In Eq. (11), it is assumed that all the excitons entering the depletion region are disassociated by the strong field ($qF_{\text{max}} a_{\text{ex}} \gg E_x$) into free electrons and holes and thus are able to contribute to the current,^{2,3} where F_{max} is the maximum field in the depletion region and a_{ex} is the exciton Bohr radius.

B. Short-circuit current

The explicit solutions for the electron and exciton concentrations under illumination and zero bias can be written as follows:

$$\Delta n_e = \frac{1}{2\sqrt{\delta}} [(\sqrt{\delta} - M_\Delta)F(L_1, D_e, G_e) - 2M_{12}F(L_1, D_x, G_x)] + [(\sqrt{\delta} + M_\Delta)F(L_2, D_e, G_e) + 2M_{12}F(L_2, D_x, G_x)], \quad (13)$$

$$\Delta n_x = \frac{1}{2\sqrt{\delta}} [(\sqrt{\delta} + M_\Delta)F(L_1, D_x, G_x) - 2M_{21}F(L_1, D_e, G_e)] + [(\sqrt{\delta} - M_\Delta)F(L_2, D_x, G_x) + 2M_{21}F(L_2, D_e, G_e)]. \quad (14)$$

Equations (13) and (14) are in fact identical to Eqs. (9) and (10), except that the mechanisms of carrier generation are different, $F(L, D, G)$ vs $\Delta n \exp(-z/L)$.

The corresponding short-circuit current is then

$$j_{\text{scc}} = qD_e \left. \frac{d\Delta n_e}{dz} \right|_{z=0} + qD_x \left. \frac{d\Delta n_x}{dz} \right|_{z=0} = qG_e \left(\frac{\eta}{L_1^{-1} + \alpha} + \frac{1 - \eta}{L_2^{-1} + \alpha} \right) + qG_x \left(\frac{\zeta}{L_1^{-1} + \alpha} + \frac{1 - \zeta}{L_2^{-1} + \alpha} \right). \quad (15)$$

The interpretation of this result is similar to that of Eq. (11). This result can be compared to that obtained without consideration of excitons:

$$j_{\text{scc0}} = \frac{qG_e}{L_e^{-1} + \alpha}. \quad (16)$$

Figure 3 shows the ratio of $j_{\text{scc}}/j_{\text{scc0}}$ for a few different doping levels. Indeed, as shown in Ref. 3, the short-circuit current can be significantly enhanced by including the exciton contribution.

Analogous to the situation for the dark-saturation current, when b is relatively large, the contribution of the L_2 component to the short-circuit current is also negligible, which means we can set all $F(L_2, D_e, G_e)$ - and $F(L_2, D_x, G_x)$ -related terms in Eqs. (13) and (14) to zero or

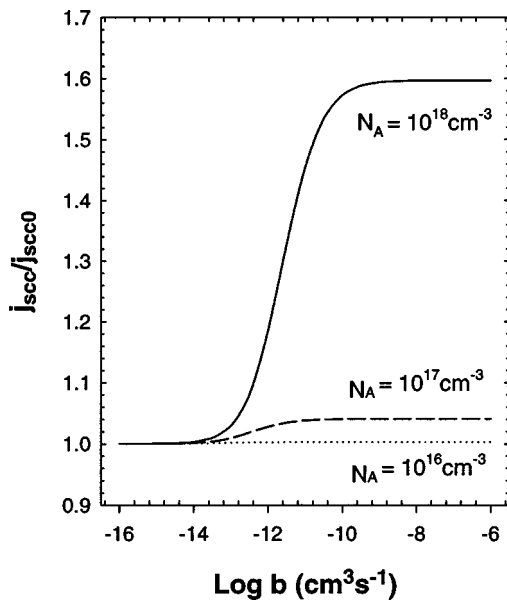


FIG. 3. Ratio of short-circuit current density with excitons considered to that with excitons neglected as a function of the exciton binding coefficient at three doping levels: $N_A = 10^{16}$, 10^{17} , and 10^{18} cm^{-3} , assuming $G_e = 10^{10} \text{ cm}^{-3} \text{ s}^{-1}$ and $G_x = 0$.

let $\eta=1$ and $\zeta=1$ in Eqs. (15). It was shown numerically in Ref. 3 that the exciton effect can significantly enhance the short-circuit current for the small b region, and the enhancement strongly depends on the fraction of the exciton generation (G_x) at a fixed total generation ($G_e + G_x$); for the large b region, there is still an enhancement, but it is independent of the partition between G_e and G_x . The reasons for their numerical results can be well explained with Eq. (15). For the small b , $\eta \rightarrow 0$ and $\zeta \rightarrow 1$, electrons and excitons mostly diffuse with diffusion lengths $L_1 \approx L_e$ and $L_2 \approx L_x$, respectively. Since $L_x > L_e$, a large fraction of G_x will certainly be beneficial. For the large b region, due to the rapid exchange, the electrons and excitons are transported as a coupled system with an effective diffusion length $L_1 > L_e$, and an enhancement is expected, but the current is given simply by $j_{\text{scc}} = q(G_e + G_x)/(L_1^{-1} + \alpha)$, independent of the partition.

Figure 4 shows a comparison between approximate and exact solutions for electron and exciton concentrations. Even for a not-so-large value of $b = 10^{-11} \text{ cm}^3 \text{ s}^{-1}$, the discrepancy is small; for $b = 10^{-9} \text{ cm}^3 \text{ s}^{-1}$, the discrepancy is invisible. It is very likely that for most of the real semiconductors, the approximate solutions are accurate enough. For instance, b is found to be on the order of $10^{-7} \text{ cm}^3 \text{ s}^{-1}$ at 300 K for Si.^{4,5} Because we have demonstrated that for the large b region, the exciton effect in the dark-saturation current is minimal, the major effect of excitons on the Si solar cell performance relies on whether the effective diffusion length L_1 is significantly greater than that of the electron L_e .

IV. SUMMARY

Using the same model as Ref. 3, we have studied the contribution of excitons on the dark-saturation current and short-circuit current of an n^+p solar cell. We have found that the effect of excitons in the dark-saturation current is very

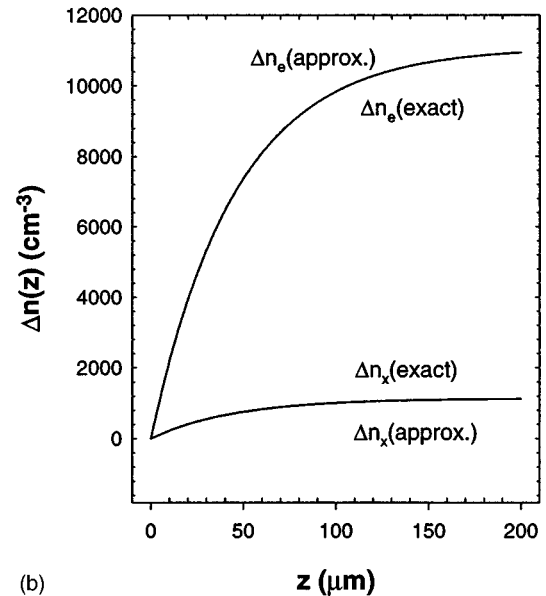
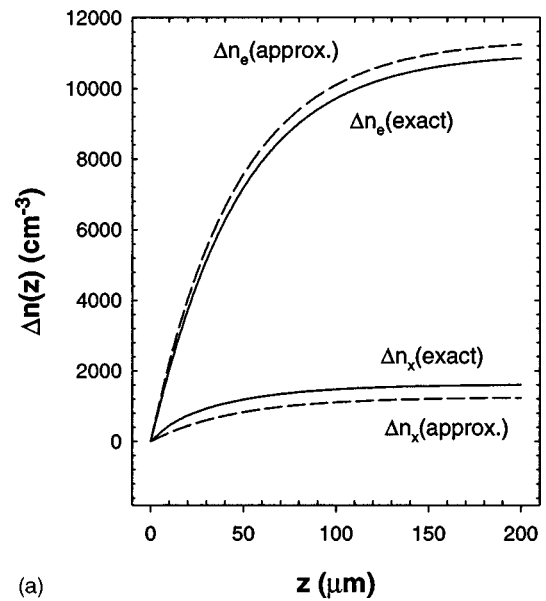


FIG. 4. Spatial distributions of excess electrons and excitons densities as functions of the distance from the edge of the depletion region, for (a) $b = 10^{-11} \text{ cm}^3 \text{ s}^{-1}$ and (b) $b = 10^{-9} \text{ cm}^3 \text{ s}^{-1}$, with $N_A = 10^{17} \text{ cm}^{-3}$, assuming $G_e = G_x = 5 \times 10^9 \text{ cm}^{-3} \text{ s}^{-1}$.

sensitive to the boundary condition for excess excitons at the edge of the depletion region. With the assumption of the near equilibrium between the electrons and excitons, we find the exciton effect is rather small and may slightly increase the dark-saturation current for large b , which is contrary to the conclusion of significant reduction in the dark-saturation current made in previous work with the assumption of no excess excitons at the edge. The results for the short-circuit current are very similar to the previous work. Compared to previous work, the analytical results for either the carrier concentrations or the corresponding currents have now been presented in a simple manner where the physical meaning of each individual term is elucidated or revealed. Furthermore, we have found, for practical purposes, very accurate approximate solutions for the carrier concentrations and correspond-

ing currents. We have arrived at an important conclusion which is that the major effect of excitons on the Si solar cell performance relies on whether the effective diffusion length L_1 is significantly greater than that of the electron L_e .

ACKNOWLEDGMENTS

This work was supported by the US Department of Energy under Contract No. DE-AC36-83CH10093. Y.Z. ac-

knowledges helpful discussions with Dr. Tihu Wang of NREL.

¹A. Hangleiter, Phys. Rev. Lett. **55**, 2976 (1985); J. Electron. Mater. **14a**, 213 (1985).

²D. E. Kane and R. M. Swanson, J. Appl. Phys. **73**, 1193 (1993).

³R. Corkish, D. S.-P. Chen, and M. A. Green, J. Appl. Phys. **79**, 195 (1996).

⁴E. L. Nolle, Sov. Phys. Solid State **9**, 90 (1967).

⁵J. Barrau, M. Heckmann, J. Collet, and M. Brousseau, J. Phys. Chem. Solids **34**, 1567 (1973).